

Joint constraints on galaxy bias and σ_8 through the N-pdf of the galaxy number density

Pablo Arnalte-Mur,^{a,b} Patricio Vielva,^c Vicent J. Martínez,^{a,b}
José L. Sanz,^c Enn Saar,^d and Silvestre Paredes^e

^aObservatori Astronòmic de la Universitat de València, C/Catedràtic José Beltrán, 2, 46980 Paterna, València, Spain.

^bDepartament d'Astronomia i Astrofísica, Universitat de València, C/Dr. Moliner 50, 46100 Burjassot, València, Spain.

^cInstituto de Física de Cantabria (CSIC-UC), Avda. de Los Castros s/n, E-39005 - Santander, Spain.

^dTartu Observatoorium, EE-61602, Tõravere, Estonia.

^eDepartamento de Matemática Aplicada y Estadística, Universidad Politécnica de Cartagena, C/Dr. Fleming s/n, 30203 Cartagena, Spain.

E-mail: pablo.arnalte@uv.es, vielva@ifca.unican.es, martinez@uv.es,
sanz@ifca.unican.es, saar@to.ee, silvestre.paredes@upct.es

Abstract. We present a full description of the N-probability density function of the galaxy number density fluctuations. This N-pdf is given in terms, on the one hand, of the cold dark matter correlations and, on the other hand, of the galaxy bias parameter. The method relies on the assumption commonly adopted that the dark matter density fluctuations follow a local non-linear transformation of the initial energy density perturbations. The N-pdf of the galaxy number density fluctuations allows for an optimal estimation of the bias parameter (e.g., via maximum-likelihood estimation, or Bayesian inference if there exists any *a priori* information on the bias parameter), and of those parameters defining the dark matter correlations, in particular its amplitude (σ_8). It also provides the proper framework to perform model selection between two competitive hypotheses. The parameters estimation capabilities of the N-pdf are proved by SDSS-like simulations (both ideal log-normal simulations and mocks obtained from Las Damas simulations), showing that our estimator is unbiased. We apply our formalism to the 7th release of the SDSS main sample (for a volume-limited subset with absolute magnitudes $M_r \leq -20$). We obtain $\hat{b} = 1.193 \pm 0.074$ and $\hat{\sigma}_8 = 0.862 \pm 0.080$, for galaxy number density fluctuations in cells of a size of $30h^{-1}\text{Mpc}$. Different model selection criteria show that galaxy biasing is clearly favoured.

Keywords: cosmology: observations – cosmology: large scale structure – galaxies: clusters – methods: data analysis – methods: statistical

Contents

1	Introduction	1
2	The galaxy number density model	2
2.1	Distribution of the galaxy number density fluctuations	3
2.2	Parameter estimation	4
2.2.1	Estimation of the uncertainty on the parameters	6
2.3	Model selection	6
3	Data	7
3.1	SDSS Main galaxy sample	7
3.2	Lognormal simulations	8
3.3	Las Damas set of mock catalogues	9
4	Tests of the method	11
4.1	Application to lognormal simulations	12
4.2	Application to Las Damas simulations	13
4.2.1	Robustness with respect to the fiducial cosmological model	15
5	Results for SDSS data	16
5.1	Model selection	19
6	Conclusions and discussions	19

1 Introduction

Observations of the distribution of the galaxies [1, 2] and state-of-the-art N-body simulations [3, 4] show that the large scale structure (LSS) of the universe forms a network of filaments, clusters and voids, mostly defined by the cold dark matter fluctuations. Galaxies trace the dark matter density field through the bias parameter, which links the evolution of the matter gravitational potential and the galaxy formation and distribution. Actually, determining the galaxy bias is not only useful to trace the dark matter structure, but also helps to understand the process of galaxy formation and distribution [5].

Depending on the galaxy type that is under consideration, different aspects of the LSS network are probed. For instance, Luminous Red Galaxies (LRGs) will be associated with dark matter halos, with the most luminous ones corresponding to large clusters (typically formed at the crossing of several filaments); spiral galaxies will be, however, better tracers for the filaments of the network, where they appear in a larger proportion; QSOs will serve as tracers of the distant universe, where galaxies are still in the phase of accretion of matter to the inner black hole; etc.

LSS surveys as NVSS [6], 2MASS [7], SDSS [1] or VIPERS [8] have provided very useful information (in a large wavelength range) about galaxy bias: e.g. [9] for the NVSS, e.g. [10] for the 2MASS, e.g. [11] for the SDSS and e.g. [12] for VIPERS. In most of the literature, the bias has been estimated using the 3D-correlation function of galaxies [13–15], counts-in-cells statistics [2, 16–18], the projected correlation function [11, 19–21], the bi-spectrum [22, 23]

and higher order moments of the galaxy distribution [5, 24–26]. The bias can also be inferred estimating the 1-point distribution function (pdf) from counts in cells, assuming a model for the mass pdf and measuring the galaxy over-density, see e.g., [12, 16] and references therein. Related, though not identical reasoning, has been used in this paper. In particular, as pointed out by Kitaura, Jasche and Metcalf in [27], it is possible to make a Bayesian matter density field reconstruction assuming a log-normal prior and modelling the galaxy distribution by a Poissonian process. The log-normal model is also adopted as a prior for the density field in inference models for large-scale structure as the one introduced by Jasche and Kitaura [28] by means of the Hamiltonian Monte Carlo (HMC) algorithm. Other approaches to determine the galaxy bias are usually based on the use of multivariate probability distributions, typically Gaussian or lognormal distributions, which are well suited priors for Bayesian analyses (see e.g. [29–32] and references therein).

Our method relies on the use of the whole set of N-pdf of the galaxy number density fluctuations. This multivariate probability density function depends on the bias parameter and the correlations of the underlying cold dark matter fluctuations. When this N-pdf is seen as a function of the bias parameter, it represents, in fact, the likelihood of the data (i.e., the galaxy catalogue) given the galaxy bias parameter. Therefore, the N-pdf provides a full description of the statistical properties of the galaxy number density field, and allows one to derive interesting bias estimators as the maximum-likelihood bias, the mean bias, etc. In addition, it also gives the opportunity of performing model selection among different galaxy biasing scenarios. Finally, our approach provides a coherent scheme for introducing any available information on the bias parameter in the form of *prior* probabilities, following the Bayes theorem.

The paper is organized as follows. In section 2 the model is presented, and it illustrates how to derive the N-pdf of the galaxy number density fluctuations (section 2.1), as well as how to perform parameter estimation (section 2.2) and model selection (section 2.3). In section 3 we present the real and simulated data used in this work: the real galaxy catalogues from the SDSS (section 3.1), a set of lognormal simulations following our model (section 3.2), and a set of mocks obtained from N-body cosmological simulations (section 3.3). We test the performance of our approach by analysing both sets of simulations in section 4. The results obtained from the application of the method to SDSS data are given in section 5. Finally, we give our conclusions in section 6.

Except when noted otherwise, we use a fiducial flat Λ CDM cosmological model with parameters $\Omega_m = 0.308$, $\Omega_\Lambda = 0.692$, $\sigma_8 = 0.8149$ based on the *Planck-2015* results [33]. All the distances used are comoving and are given in terms of the Hubble parameter $h = H_0/100 \text{ kms}^{-1}\text{Mpc}^{-1}$.

2 The galaxy number density model

As outlined in the Introduction, we aim to determine the N-pdf of the galaxy number density field, given the correlation properties of the dark matter density field, as well as the bias parameter b , that relates the galaxy formation with the fluctuations of the dark matter density field.

The description of the galaxy density field via its N-pdf provides a powerful framework to derive detailed statistical analyses. In particular, the N-pdf allows for a maximum-likelihood estimation (or Bayesian estimation, in the case of introducing any possible prior knowledge)

of the parameters describing the galaxy distribution. In addition, model selection approaches can be also applied.

These two approaches have been applied by [34, 35] to the N-pdf of a local Gaussian deviation of the cosmic microwave background temperature fluctuations. This deviation was given in terms of a non-linear perturbative expansion of a Gaussian field. In the Sachs-Wolfe regime, and under certain conditions, this perturbative model defaults on the weak non-linear coupling inflationary model [e.g., 36].

2.1 Distribution of the galaxy number density fluctuations

Let us denote by $\rho_{0,i}$, the initial energy density at a given position i , and by $\rho_{0,b}$ the mean initial energy density or the *background* initial energy density. Then, the *initial energy density fluctuation* at position i is nothing but:

$$\delta_{0,i} = \frac{\rho_{0,i} - \rho_{0,b}}{\rho_{0,b}}, \quad (2.1)$$

and the *initial energy density contrast* is defined as:

$$\Delta_{0,i} = 1 + \delta_{0,i} = \frac{\rho_{0,i}}{\rho_{0,b}}. \quad (2.2)$$

Trivially, $\langle \delta_{0,i} \rangle \equiv 0$ and $\langle \Delta_{0,i} \rangle \equiv 1$. As predicted by the standard inflation scenario [e.g. 37], the probability density function of the initial energy density fluctuations follows a multivariate normal distribution:

$$f(\delta_{0,i}) = \frac{1}{(2\pi)^{N/2} |\mathbf{C}_0|^{1/2}} \exp \left(-\frac{1}{2} \delta_{0,i} C_{0,ij}^{-1} \delta_{0,j} \right), \quad (2.3)$$

where N represents the number of positions (assuming a given discretization or pixelization of space) in which the field is realized, and the \mathbf{C}_0 matrix provides the Gaussian field correlations (i.e., $\langle \delta_{0,i} \delta_{0,j} \rangle \equiv C_{0,ij}$). Hereinafter, addition over repeated indices is assumed, i.e., $\delta_{0,i} C_{0,ij}^{-1} \delta_{0,j} \equiv \sum_{i=1}^N \sum_{j=1}^N \delta_{0,i} \delta_{0,j} C_{0,ij}^{-1}$.

N-body simulations have been showing, since the mid 80s, that the dark matter density field shows a non-Gaussian behaviour, even when the seeds of the initial energy density perturbations are Gaussian [e.g., 38–41]. This non-Gaussianity is a reflection of the non-linear nature of the gravitational instability. This hint provided by N-body simulations is also confirmed by large-scale surveys, that also demonstrate that the galaxy number density follows a non-Gaussian distribution. Among all the local non-linear transformations, the log-normal model [e.g., 42, 43] provides an excellent description for the galaxy distribution, at least for the lowest non-linear orders. This model also provides an excellent framework to derive analytical expressions, and it is the one adopted in this work. It is convenient to express the matter density contrast $\Delta_{m,i}$ as a function of the initial energy density fluctuations through the following transformation:

$$\Delta_{m,i} = \exp \left(\alpha \frac{\delta_{0,i}}{\sigma_{\Delta_0}} - \frac{\alpha^2}{2} \right), \quad (2.4)$$

where α is a constant and $\sigma_{\Delta_0}^2 \equiv C_{0,ii} \equiv \langle \delta_{0,i}^2 \rangle$. Conversely, the local inverse transformation is given by:

$$\delta_{0,i} = \frac{\sigma_{\Delta_0}}{\alpha} \left(\log \Delta_{m,i} + \frac{\alpha^2}{2} \right). \quad (2.5)$$

Attending to these definitions, it is straightforward to show that:

$$\begin{aligned}\alpha^2 &= \log(1 + \sigma_{\Delta_m}^2) \\ \langle \Delta_{m,i} \rangle &= 1 \\ \langle \Delta_{m,i} \Delta_{m,j} \rangle &= \exp \left[\left(\frac{\alpha}{\sigma_{\Delta_0}} \right)^2 C_{0,ij} \right] \\ H_{0,ij} &= \log(1 + C_{m,ij}),\end{aligned}\tag{2.6}$$

where $\sigma_{\Delta_m}^2 \equiv C_{m,ii}$, and $H_{0,ij} \equiv \left(\frac{\alpha}{\sigma_{\Delta_0}} \right)^2 C_{0,ij}$. Given equations (2.3) and (2.5), it is trivial to compute the N-pdf associated with the cold dark matter density field:

$$f(\Delta_{m,i}) = \frac{1}{(2\pi)^{N/2} |\mathbf{H}_0|^{1/2}} \frac{\exp \left(-\frac{1}{2} y_i H_{0,ij}^{-1} y_j \right)}{\prod_{j=1}^N \Delta_{m,j}},\tag{2.7}$$

where we have defined the auxiliary parameters y_i as

$$y_i \equiv \log \left(\Delta_{m,i} \sqrt{1 + \sigma_{\Delta_m}^2} \right).\tag{2.8}$$

The galaxy number density fluctuations $(\delta_{g,i})$ are assumed to be related to the cold dark matter density through a local transformation in terms [44, 45] of the *galaxy bias* b :

$$\delta_{g,i} = b \delta_{m,i} \implies \Delta_{m,i} = \frac{\Delta_{g,i} + b - 1}{b},\tag{2.9}$$

where $\Delta_{g,i}$ is the galaxy number density contrast. Given this relation, and taking into account equation (2.7), it is straightforward to compute the N-pdf associated with the galaxy number density field:

$$f(\Delta_{g,i}) = \frac{1}{(2\pi)^{N/2} |\mathbf{H}_0|^{1/2}} \frac{\exp \left(-\frac{1}{2} y_i H_{0,ij}^{-1} y_j \right)}{\prod_{j=1}^N (\Delta_{g,j} + b - 1)},\tag{2.10}$$

where we can use equations (2.8) and (2.9) to express y_i in terms of the galaxy number density fluctuations $(\delta_{g,i})$ and their correlations $(\mathbf{C}_g = b^2 \mathbf{C}_m)$:

$$y_i = \log \left[\frac{\sqrt{b^2 + \sigma_{\Delta_g}^2}}{b^2} (\Delta_{g,i} + b - 1) \right]\tag{2.11}$$

where $\sigma_{\Delta_g}^2 \equiv C_{g,ii} = b^2 C_{m,ii}$.

2.2 Parameter estimation

In the context of parameter estimation, the N-pdf given by equation (2.10) can be seen as the likelihood function of observations (the values of the galaxy number density contrast $\Delta_{g,i}$ at N positions in space) given a galaxy clustering model. This clustering model has two parts: on one hand the galaxy bias parameter b , and on the other the covariance of the matter fluctuations \mathbf{C}_m fixed by the cosmological model. These covariances are defined as $C_{m,ij} = \langle \delta_{m,i} \delta_{m,j} \rangle$, and are therefore equal to

$$C_{m,ij} = \xi_m(r_{ij}),\tag{2.12}$$

where r_{ij} is the comoving distance between the centers of the cells i, j , and $\xi_m(r)$ is the matter correlation function predicted by the cosmological model, filtered to account for the finite size of the cells. In our case, given a model we obtain the matter power spectrum $P_m(k)$ using the CAMB¹ software [46], and calculate the corresponding $\xi_m(r)$ via a Fourier transform using FFTLOG [47].

In the simplest case we can assume that the cosmological model is known, fixing \mathbf{C}_m , so the only free parameter is the bias b . In this case, we can express the likelihood as

$$L(\Delta_{g,i}|b) \equiv f(\Delta_{g,i}). \quad (2.13)$$

The advantages of exploiting the N-pdf for statistical analyses, as parameter estimation or model selection, are clear. In particular, given the $\Delta_{g,i}$ observed by a galaxy survey and the \mathbf{C}_m from the assumed cosmological model, we can obtain the maximum-likelihood estimate of galaxy the bias \hat{b} , as well as alternative estimates like the mean value. In addition, if any *a priori* information on the bias parameter $p(b)$ is available, it can be used together with equation (2.10) to provide the posterior probability of the bias parameter given the observations $p(b|\Delta_{g,i})$, following the Bayes' theorem:

$$p(b|\Delta_{g,i}) \propto L(\Delta_{g,i}|b) p(b). \quad (2.14)$$

This posterior probability allows performing a full Bayesian parameter estimation, as well as Bayesian model selection (e.g., Bayesian evidence).

In addition to the bias, we can also use this likelihood approach to constrain the parameters of the cosmological model via the covariance matrix for matter fluctuations, \mathbf{C}_m . In particular, we focus here on constraining the amplitude of the matter power spectrum, jointly with the galaxy bias b . We parameterize this amplitude using the standard parameter σ_8 .² In order to introduce this additional parameter in equation (2.10), we first assume a fiducial value σ_8^{fid} and compute the corresponding covariance matrix $\mathbf{C}_m^{\text{fid}}$. The covariance matrix then depends on σ_8 as

$$\mathbf{C}_m = \left(\frac{\sigma_8}{\sigma_8^{\text{fid}}} \right)^2 \mathbf{C}_m^{\text{fid}}. \quad (2.15)$$

Introducing this expression for \mathbf{C}_m into equation (2.10), we can then interpret $f(\Delta_{g,i})$ as the likelihood of the data $\Delta_{g,i}$ given the two parameters (b, σ_8) ,

$$L(\Delta_{g,i}|b, \sigma_8) \equiv f(\Delta_{g,i}). \quad (2.16)$$

In the same way as in the single-parameter case, this likelihood function can be used to obtain the joint maximum likelihood estimates for the two parameters \hat{b} , $\hat{\sigma}_8$ or other estimates. We can also combine this likelihood with any prior on the parameters to obtain the joint posterior probability distribution,

$$p(b, \sigma_8|\Delta_{g,i}) \propto L(\Delta_{g,i}|b, \sigma_8) p(b, \sigma_8). \quad (2.17)$$

In this work we always use flat wide priors either on b (for equation 2.14) or on (b, σ_8) (for equation 2.17), so these relations are just a *normalization* of the posterior distributions.

¹<http://camb.info>

² σ_8^2 corresponds to the matter density variance in spheres of radius $R = 8h^{-1}$ Mpc, when using a linear model extrapolated to $z = 0$.

However, these prior probabilities could be used, e.g., to add information coming from independent observations constraining σ_8 .

In principle, these two parameters could be degenerate, as they are both related to the overall galaxy clustering amplitude. This is the case in the analyses of galaxy bias based on two-point statistics, where the estimates of b are completely degenerate with σ_8 , and in fact one can only constrain the quantity $b\sigma_8$. When using the N-pdf, however, we also have information on the shape of the distribution that breaks this degeneracy. Our model predicts a multivariate log-normal N-pdf for the matter density contrast $\Delta_{m,i}$, (eq. 2.7), but a different distribution for the galaxy density contrast $\Delta_{g,i}$ (eq. 2.10) when $b \neq 1$. Therefore, variations in σ_8 change the overall variance of the distribution, while keeping the log-normal shape, while variations in b change both the overall variance and the shape of the distribution, breaking the degeneracy.

One could also use this approach to constrain other cosmological parameters that affect the model covariance matrix \mathbf{C}_m , such as Ω_m . However, these parameters affect as well the estimation of the galaxy density $\Delta_{g,i}$ from the data, via the conversion from galaxy redshifts to distances. This means that the simple likelihood interpretation presented here is not valid in this case. For this reason, we keep all cosmological parameters except σ_8 fixed in our analysis. In section 4.2 we test the reliability of the method to this assumption.

2.2.1 Estimation of the uncertainty on the parameters

As described above, we can use the N-pdf of the galaxy density field to derive the maximum-likelihood estimation of the parameters b, σ_8 . We estimate the uncertainty on these parameters using the Fisher matrix (\mathbf{F}) formalism.

In the case in which we keep σ_8 fixed and only fit for the bias b , the uncertainty $\sigma_{\hat{b}}$ on our estimate \hat{b} is given by

$$\sigma_{\hat{b}}^2 = \mathbf{F}_{\hat{\mathbf{b}}}^{-1} ; \quad \mathbf{F}_{\hat{\mathbf{b}}} = - \left[\frac{\partial^2 \ell_b}{\partial b^2} \right]_{b=\hat{b}}, \quad (2.18)$$

where $\ell_b = \log L(\Delta_{g,i}|b)$. In the case in which we estimate both b and σ_8 from our method, the covariance matrix $\mathbf{C}_{\hat{b}, \hat{\sigma}_8}$ of the estimated parameters $\hat{b}, \hat{\sigma}_8$ is given by

$$\mathbf{C}_{\hat{b}, \hat{\sigma}_8} = \mathbf{F}_{\hat{\mathbf{b}}, \hat{\sigma}_8}^{-1} ; \quad \mathbf{F}_{\hat{\mathbf{b}}, \hat{\sigma}_8} = - \left[\begin{array}{cc} \frac{\partial^2 \ell}{\partial b^2} & \frac{\partial^2 \ell}{\partial b \partial \sigma_8} \\ \frac{\partial^2 \ell}{\partial \sigma_8 \partial b} & \frac{\partial^2 \ell}{\partial \sigma_8^2} \end{array} \right]_{(b, \sigma_8) \equiv (\hat{b}, \hat{\sigma}_8)}, \quad (2.19)$$

where in this case $\ell = \log L(\Delta_{g,i}|b, \sigma_8)$. The diagonal terms of this matrix correspond to the variances of the estimated parameters

$$\sigma_{\hat{b}} = \sqrt{C_{11}} ; \quad \sigma_{\hat{\sigma}_8} = \sqrt{C_{22}}, \quad (2.20)$$

while the diagonal term corresponds to the covariance between the two parameters.

2.3 Model selection

Even if *a priori* information on b is lacking, model selection can also be performed following a likelihood-based approach. In the context of the N-pdf of the galaxy density field, it is interesting to compare our full two-parameter model (defined by equations 2.15 and 2.16) to

an alternative no bias scenario (i.e., $b \equiv 1$) in which we only fit for σ_8 . In this work, we consider the *Akaike information criterion* [AIC, 48], the *Bayesian information criterion* [BIC, 49], and the *generalized likelihood ratio test* (GLRT). These criteria have been already applied (and explained in detail) in the context of a N-pdf derived for a non-Gaussian model describing a local transformation [34], that could represent the weak non-linear coupling inflationary model [36], in the Sachs-Wolfe regime. Given a certain hypothesis H_α , defined both by the maximum-likelihood parameters θ_α ³ and a maximum log-likelihood value $\ell_\alpha \equiv \log L(\Delta_{g,i}|\theta_\alpha)$, the AIC and BIC are given by:

$$\mathbf{AIC}(H_\alpha) = 2(N_p - \ell_\alpha) \quad (2.21)$$

$$\mathbf{BIC}(H_\alpha) = 2\left(\frac{N_p}{2} \log N - \ell_\alpha\right) \quad (2.22)$$

where N_p is the number of free parameters in the model (in our case, either $N_p = 1$ or $N_p = 2$), and N is the number of data points (in our case, the number of grid points in which we computed Δ_g). Therefore, for instance, a given hypothesis H_α is said to be favoured by the **AIC** with respect to an alternative H_β , if $\mathbf{AIC}(H_\alpha) < \mathbf{AIC}(H_\beta)$. The same is applied to the **BIC** model selection procedure. Regarding the GLRT approach, H_α is said to be favoured over H_β , at a ν level (with $\nu > 0$), if $\log\left(\frac{L_\alpha}{L_\beta}\right) \geq \nu$.

3 Data

In this section, we present the different data sets used in this work. In section 3.1 we explain the selection of our sample from the SDSS, and how we estimate the galaxy density field from it. Section 3.2 describes how we generated a set of log-normal simulations to test the consistency of our method. Finally, in section 3.3 we present the Las Damas set of mocks which we used to test the method in realistic simulations.

3.1 SDSS Main galaxy sample

We use the method described in section 2 to study the galaxy bias and matter power spectrum amplitude for a galaxy sample drawn from the 7th data release [50] of the SDSS main catalogue. We used the data provided by the New York University Value Added Catalogue [NYU-VAGC, 51]. In order to avoid problems due to the radial selection function, we selected a volume limited sample with $M_r \leq -20$ in the redshift range $0.033 < z < 0.106$, where M_r is the $K + E$ corrected r -band absolute magnitude. We chose this redshift range to ensure that the sample is volume limited, and also to use a sample consistent with the correlation function analysis of [11] and the Las Damas mocks (see section 3.3). We convert the measured angles and redshifts into co-moving coordinates using our fiducial cosmological model based on the *Planck-2015* results.

In order to study the N-pdf as described in section 2, we need to estimate from this galaxy sample the galaxy overdensity field Δ_g . We chose to study this field using a grid of cubic cells covering the volume of the survey. In order to choose the physical size of the cells, we studied the variance between cells obtained at different resolutions. Comparing to the variance obtained for Poisson catalogues of the same volume and density, we can quantify the relative effect of shot noise. Using this approach, we decided to adopt cubic cells with a side

³in our case, depending of the model, $\theta = b$ or $\theta = (b, \sigma_8)$

of $30 h^{-1} \text{ Mpc}$, for which the observed variance is ~ 7 times larger than the Poisson noise, so we can assume that we are in the signal-dominated regime.

Once our grid of cells is defined, we proceed as follows to estimate Δ_g . In the first place, we compute the completeness for each of the cells (c_i) as the combination of two components: the radial and the angular selection functions. For the former we assume a constant selection in the redshift range mentioned above, and for the latter we use the angular mask from the NYU-VAGC in the MANGLE software format [52, 53]. To simplify the selection function, we consider only the North Cap of the SDSS area. We use in our analysis only cells with a completeness $c_i \geq 0.8$. This leaves us with $N = 582$ valid cells, with a volume of $V = 15.7 \times 10^6 h^{-3} \text{ Mpc}^3$, embedded in a box of $240 \times 480 \times 240 h^{-3} \text{ Mpc}^3$. The total number of galaxies in the selected cells is $N_g = 90,634$.

We obtain the number of cells n_i in each of these accepted cells, and estimate the galaxy number density for each cell as

$$\rho_{g,i} = \frac{n_i}{c_i V_c} \quad (3.1)$$

where $V_c = (30 h^{-1} \text{ Mpc})^3$ is the volume of a cell. We finally compute the galaxy density contrast $\Delta_{g,i}$ normalising $\rho_{g,i}$ by the mean galaxy density (eq. 2.2). In Figure 1 we show a 3D projection of this galaxy density field obtained from the SDSS data. The galaxy density contrast field $\Delta_{g,i}$ in the N cells estimated in this way is the quantity whose pdf is given by equation (2.10). As we already take into account the selection function here to define the ‘valid’ cells, and to estimate the density, the method described in section 2 can be applied directly. We only have to take into account the positions of the selected cells to calculate the model covariance matrix \mathbf{C}_m .

3.2 Lognormal simulations

In order to test the method, we created a set of 100 lognormal realizations of the matter density field. These simulations are created following the same model described in section 2, and with the same survey geometry as the SDSS data (section 3.1), so they can be used to assess the consistency of our method. The input matter power spectrum $P_m(k)$ for these simulations corresponds to the best-fit model to the temperature + lensing *Planck-2015* data [33, table 4, column 2], computed using the CAMB software.

We generate the lognormal simulations using the method described in [54] (which is equivalent to the one in [55]), which is based on the fact that a lognormal random field is a local transformation of a Gaussian field. We compute the matter correlation function $\xi_m(r)$ via a Fourier transform of $P_m(k)$. We obtain the correlation function for the initial Gaussian field $\xi_0(r)$ using the transformation in equation (2.6), as

$$\xi_0(r) = \left(\frac{\sigma_{\Delta_0}}{\alpha} \right)^2 \log(1 + \xi_m(r)), \quad (3.2)$$

and the corresponding power spectrum $P_0(k)$ as its inverse Fourier transform. We then generate the Gaussian random field $\delta_{0,i}$ in a cubic grid using the standard method of generating Gaussian Fourier modes with variances given by $P_0(k)$ and then performing a Fast Fourier Transform (see e.g. section 7.4.1 of [56]). Finally, we obtain the corresponding matter density field $\Delta_{m,i}$ using the transformation given by equation (2.4).

To avoid possible boundary problems, we initially generate each of these lognormal simulations in a box of $(1440 h^{-1} \text{ Mpc})^3$, with cells of side $30 h^{-1} \text{ Mpc}$. We then use the cell completeness defined for the SDSS data to define the same geometry with $N = 582$ valid cells,

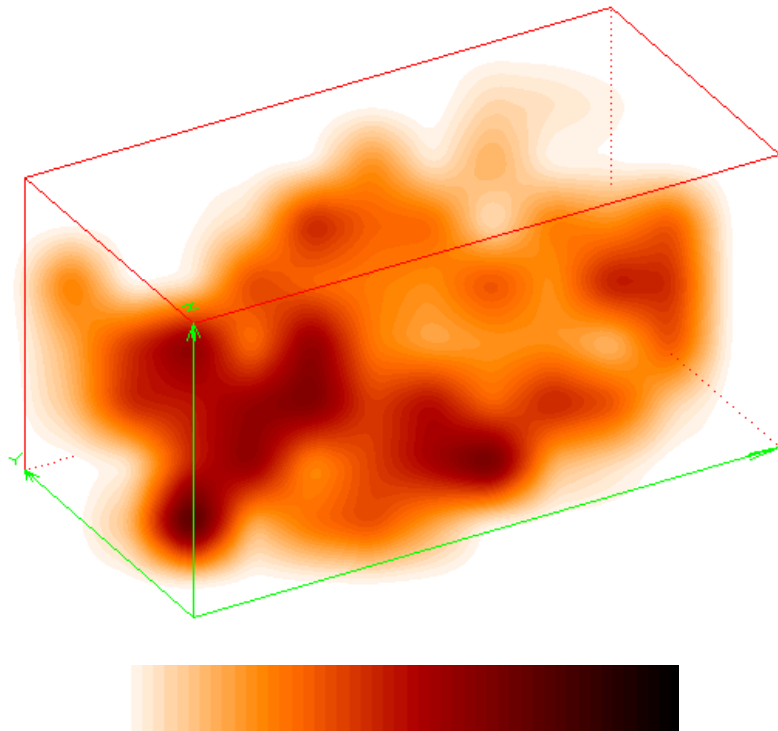


Figure 1. 3D projection of the galaxy number density field corresponding to the SDSS catalogue used in this work. The colour palette used in the projection is shown at the bottom and corresponds to densities $1 \leq \Delta_g \leq 2$ from left to right.

and we keep only the value of the density field $\Delta_{m,i}$ in those cells. In this way, we ensure that the grid points we use are always at a distance $\geq 480 h^{-1}$ Mpc from any of the borders of the box.

For each of our 100 simulations of the matter density field $\Delta_{m,i}$, given a value for the galaxy bias b , we can generate the corresponding galaxy density field $\Delta_{g,i}$ using equation (2.9). In section 4.1 we will explore the results we obtain for four input values of the bias: $b = 0.5, 1.0, 1.5, 2.0$. In Figure 2 we represent 3D-projections of the galaxy number density field for these bias values obtained from one of our simulations (therefore the underlying realization of matter fluctuations is the same for the 4 cases shown). It can be seen that, as it is expected, the clustering increases when the bias parameter is getting larger. We can compare this projection to that of the real data shown in Figure 1.

3.3 Las Damas set of mock catalogues

As a further assessment of the N-pdf method, it is important to test it in more realistic simulated catalogues, which reproduce the observed distribution of galaxies. We chose to use the set of galaxy mocks obtained from the Las Damas simulations⁴ [57, 58], and in particular the *gamma* release. These mock catalogues were created matching both the selection effects and the clustering properties of the SDSS-DR7 real catalogues, and are therefore optimal for

⁴<http://lss.phy.vanderbilt.edu/lasdamas/>

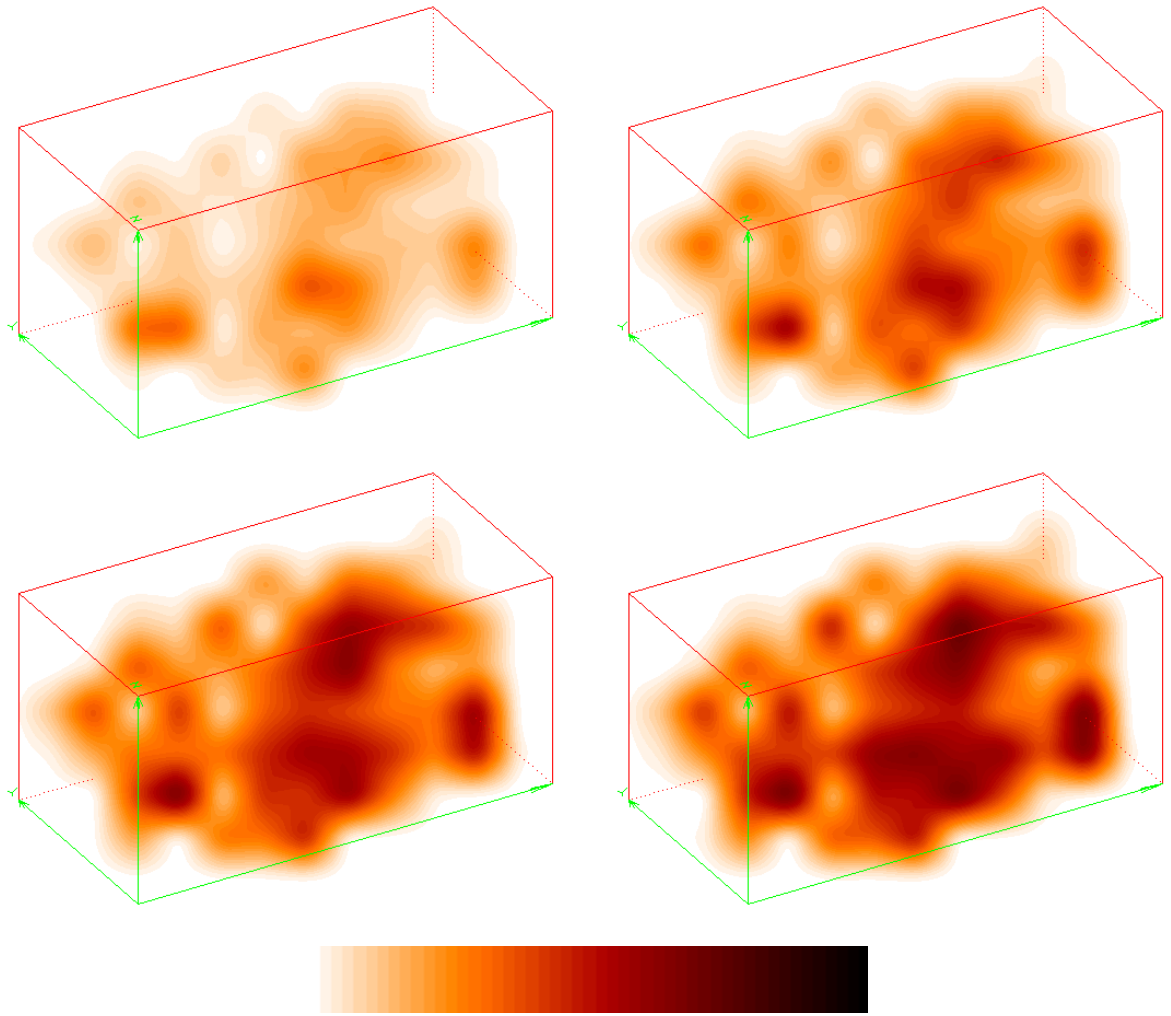


Figure 2. Galaxy number density field, shown as a 3D projection, for one of the realizations of the lognormal simulations. The underlying cold dark matter density field is the same for all the cases, but the galaxy bias is different in each of the panels. Bias values are, from left to right and top to bottom, $b = 0.5, 1.0, 1.5, 2.0$. The colour palette used in the projection is the same as in Figure 1. Notice how clustering increases as bias grows.

our purposes. We use the set of mocks corresponding to the galaxy selection $M_r \leq -20$, to match the SDSS galaxy catalogue described in section 3.1.

The mocks used here were obtained from the Esmeralda dark matter simulation: a set of 30 N-body realizations, each containing 1250^3 particles in a volume of $(640 h^{-1} \text{ Mpc})^3$. These realizations are created using a standard ΛCDM model with parameters $\Omega_m = 0.25$, $\Omega_\Lambda = 0.75$, $\sigma_8 = 0.8$. We use this same cosmological model when analysing the Las Damas mocks.

The simulations are populated by galaxies using the halo occupation distribution (HOD) formalism, with the HOD parameters tuned to reproduce the observed number density and projected correlation function $w_p(r_p)$ (at scales $r_p \in [0.3, 30] h^{-1} \text{ Mpc}$, as studied in [11]) of the corresponding SDSS catalogues. Finally, the mock galaxy catalogues are obtained

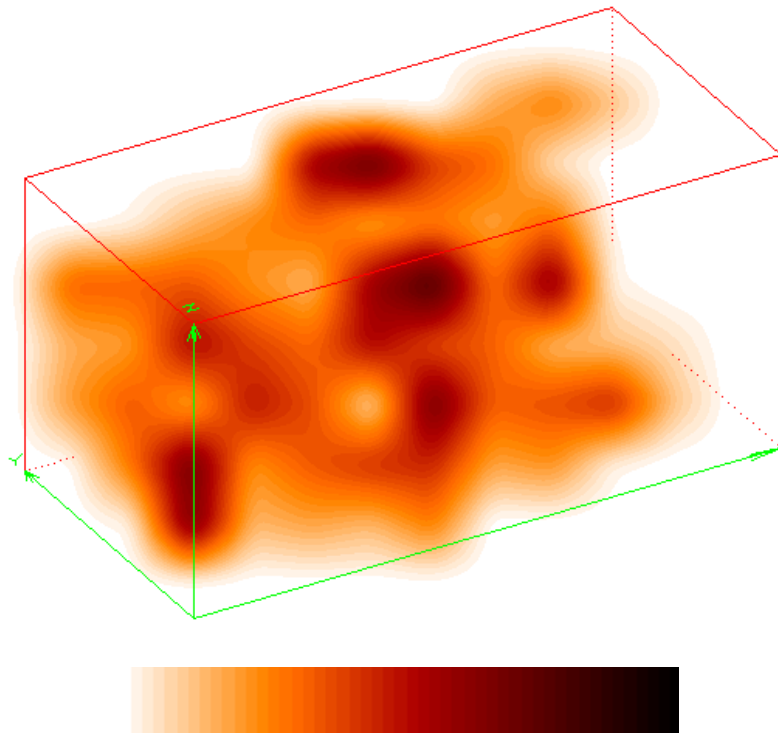


Figure 3. 3D projection of the galaxy number density field corresponding to one of the Las Damas mocks. The colour palette used in the projection is the same as in Figures 1 and 2. Notice the similarity of the clustering in this case and that of the real data shown in Figure 1.

by applying the SDSS angular selection mask from NYU-VAGC and appropriate redshift limits. Both selections match those we used to select the real SDSS catalogue presented in section 3.1. We use the *North-only* version of the mocks for which four non-overlapping mocks are obtained from each simulation box. Hence, we end up with a total of 120 mock galaxy catalogues.

For each of the mocks, we compute the galaxy density field $\Delta_{g,i}$ using the same method described in section 3.1 for the SDSS data, including the use of the angular and radial selection functions, and keeping only cells with completeness $c_i \geq 0.8$. For consistency, we use here the same cosmological model used to create the simulations (which is slightly different from the *Planck-2015* model we use elsewhere). This results in a slightly different number of valid cells ($N = 589$) with respect to the SDSS data catalogue. In section 4.2 we use the Las Damas mocks to test the reliability of our method with respect to the cosmological model used here. In Figure 3 we show a 3D projection of the galaxy density field for one of the Las Damas mocks. By comparing to Figure 1 we see that the clustering of the mock seems very similar to that of the real data.

4 Tests of the method

We tested the N-pdf method to constrain b , σ_8 presented in section 2 using the two sets of simulated galaxy density fields presented in sections 3.2 and 3.3. First, in section 3.2 we

show the results of applying our method to the lognormal simulations generated using this same model for the density field. This is a way to assess the internal consistency of the method. Then, in section 4.2, we analyse the Las Damas mock catalogues. In this case, we can assess the reliability of the method in a realistic case when the basic assumptions (lognormal distribution of matter, linear biasing) are approximate but not exactly fulfilled.

4.1 Application to lognormal simulations

We investigated the performance of the N-pdf method presented in section 2 in the ideal case represented by the lognormal simulations described in section 3.2. In this way, we test the internal consistency of the method and, at the same time, we check whether the maximum-likelihood parameter estimator is, in fact, unbiased, and we explore how the estimator sensitivity depends on the actual bias factor. We apply the method to the 100 simulations, for galaxy density fields generated with four different values of the true bias: $b_{\text{true}} = 0.5, 1.0, 1.5, 2.0$.

First, we applied the method to the simulated fields assuming that the cosmological model was fully known, so that \mathbf{C}_m was kept fixed to the true values of the matter correlation function, and we only fit for the galaxy bias b . In Figure 4 we present the histograms of the values of \hat{b} recovered for each realization. Each panel of the figure corresponds to a different value of the true bias. In each panel, we list the mean value of our maximum-likelihood estimate \hat{b} , together with its dispersion in the 100 simulations. For each simulation, we also estimate the Fisher matrix uncertainty on the bias according to equation (2.18). We also list in each panel the mean value and dispersion of the $\sigma_{\hat{b}}$ obtained in this way.

We notice first that, as expected, the bias estimation is unbiased and that, second, the error associated to the parameter estimation is very well described by the Fisher matrix. Finally, the parameter dispersion increases as the bias increases, but the relative error in the bias determination (i.e., $\sigma_{\hat{b}}/\hat{b}$) is almost constant for all the cases: $\approx 2.3\%$.

As a second step, we perform the fit in both the galaxy bias b and the power spectrum amplitude σ_8 , as described by equations (2.15) and (2.16). We show the 2D distribution of the maximum-likelihood values $(\hat{b}, \hat{\sigma}_8)$ obtained from the 100 realisations in Figure 5, together with the marginal distributions of each of the two parameters. As before, each of the panels corresponds to a different true value of the bias. We also obtained in each case the parameter covariance matrix and the corresponding uncertainties using the Fisher matrix approach described in section 2.2.1. In each panel, we show as a dashed contour the 1σ ellipse derived from the mean covariance matrix, and list the mean and dispersion of both the parameter estimations and their uncertainties.

We obtain, again, that the maximum-likelihood estimators of both b and σ_8 are unbiased. For the case of the bias, we obtain again that the Fisher matrix estimation of the uncertainty matches the observed dispersion of \hat{b} . As in the first case, this uncertainty scales with the bias, although it is significantly larger now, with $\sigma_{\hat{b}}/\hat{b} \approx 6.7\%$. This is understandable, as now there is additional freedom due to the value of σ_8 being allowed to change. Regarding the uncertainty on σ_8 , we see that the Fisher matrix approach slightly over-estimates it (by a $\approx 9\%$). Hence, we can take it as a conservative uncertainty estimate. We also observe that the error on $\hat{\sigma}_8$ does not depend on the (true) value of the bias.

From the analysis of the lognormal simulations, we can conclude that our method is consistent, in the sense that, when its assumptions are fulfilled, it provides unbiased estimates of b and σ_8 . Moreover, the Fisher matrix approach provides correct (or slightly conservative) estimates of the uncertainty.

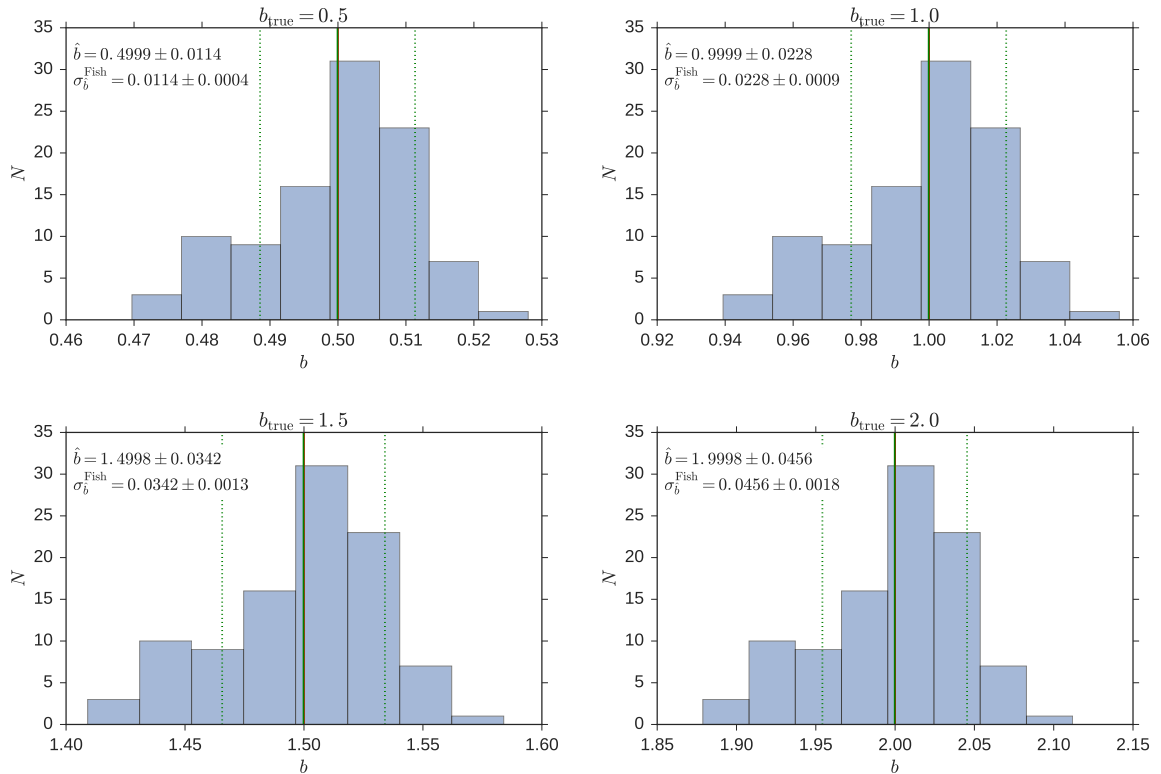


Figure 4. Distribution of the maximum-likelihood estimates of the bias \hat{b} , for the 100 lognormal simulations, for the case in which the amplitude of the matter power spectrum is fixed. Each of the panel corresponds to a different value of the true bias in the simulations. From left to right and top to bottom, these values are $b_{\text{true}} = 0.5, 1.0, 1.5, 2.0$. Input values are given as vertical red lines, whereas the mean \hat{b} over the simulations are represented by solid vertical green lines. The dashed green lines encompass the 1σ region around the mean. We note in each case the mean \hat{b} and the mean uncertainty $\sigma_{\hat{b}}$ obtained via the Fisher matrix.

4.2 Application to Las Damas simulations

To further test the reliability of the N-pdf method, and its applicability to the real distribution of galaxies in the Universe, we applied it to the Las Damas mocks described in section 3.3, which provide a test bench closely matching the galaxy distribution in the SDSS catalogue. We first applied the method, both fitting only for the bias and for both the bias and the amplitude σ_8 , using as fiducial model the true cosmological model used to create the simulations (see section 3.3). Regarding the input value of b for the simulations, we know that they were built to match the projected correlation function of the real SDSS data. We therefore take as the ‘true’ bias the value of $b = 1.20 \pm 0.01$ obtained by [11] for the corresponding SDSS catalogue⁵ by a HOD fit to $w_p(r_p)$. We note that other fitting methods in that same work gave compatible values of the bias with significantly larger error.

The results of the application of the N-pdf method to the Las Damas mocks are shown in Figure 6. The left panel shows the distribution of maximum-likelihood estimates of the bias, \hat{b} , when we keep all the cosmological parameters fixed to their true values. In this case,

⁵The analysis in [11] uses the same Las Damas cosmology, so we can use this value directly in our comparison

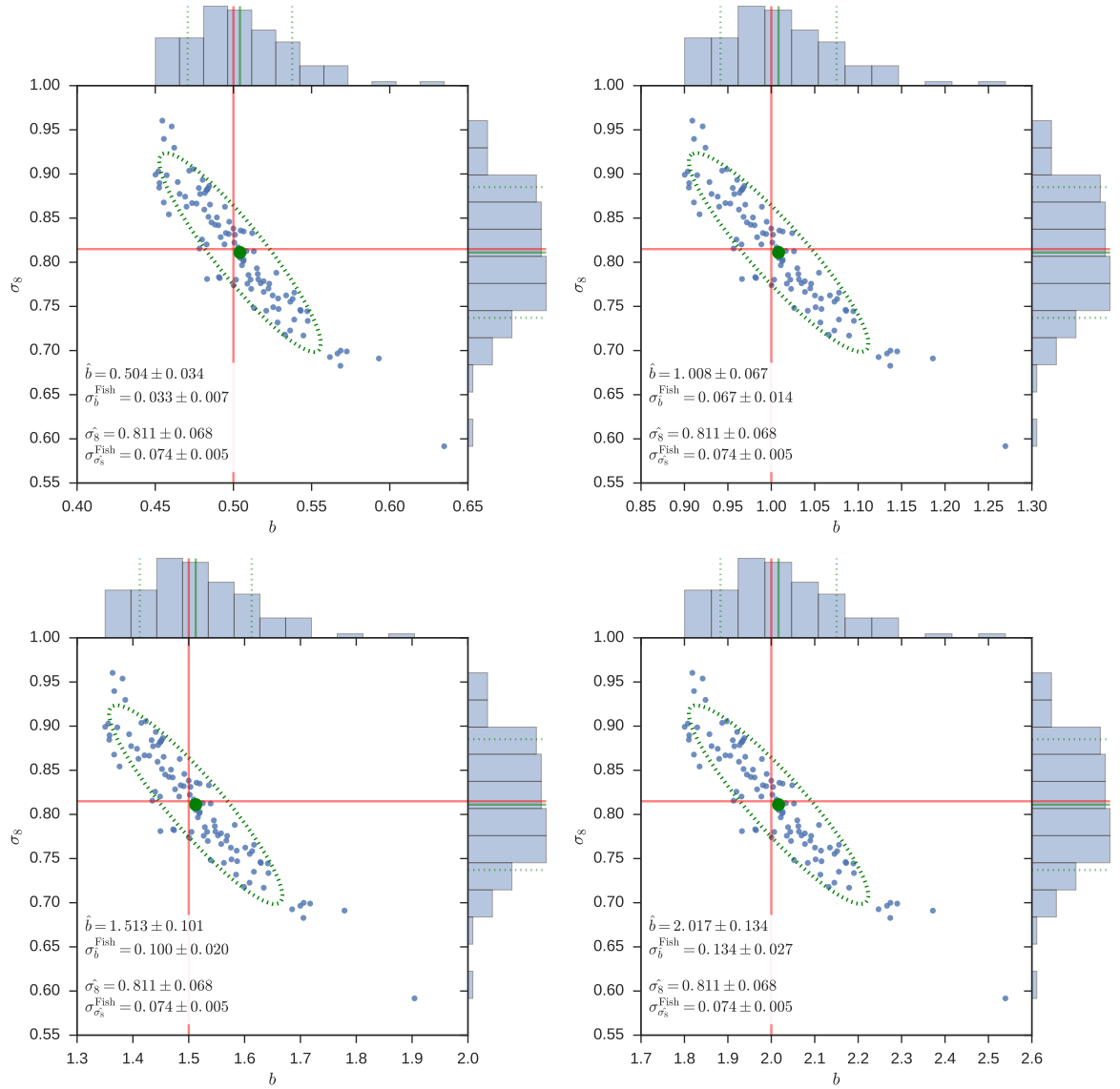


Figure 5. Distribution of the maximum-likelihood estimates of the parameters b , σ_8 , for the 100 lognormal simulations, for the case in which we allow both parameters to change. From left to right and top to bottom, the panels correspond to different values of the true bias: $b_{\text{true}} = 0.5, 1.0, 1.5, 2.0$. Blue dots represent the individual estimates for each realization and the histograms at the top and right of each panel show the marginal distributions for each parameter. Input values are given as red lines. The big green dot and solid lines correspond to the mean of the recovered parameters over the simulations. The dashed green lines in the histograms encompass the 1σ regions around the mean for each parameter. The green dashed ellipse represents the joint 1σ region corresponding to the mean covariance matrix from the Fisher matrix approach.

we obtain the estimates of the bias $\hat{b} = 1.2133 \pm 0.0277$. The uncertainties derived via the Fisher matrix are $\sigma_{\sigma_8}^{\text{Fish}} = 0.0271 \pm 0.0008$, which provide again a very good estimate of the true dispersion of the recovered \hat{b} . The relative error on the estimated bias, $\sigma_{\hat{b}}/\hat{b} = 2.3\%$ is remarkably close to the one obtained for the lognormal simulations in the previous section.

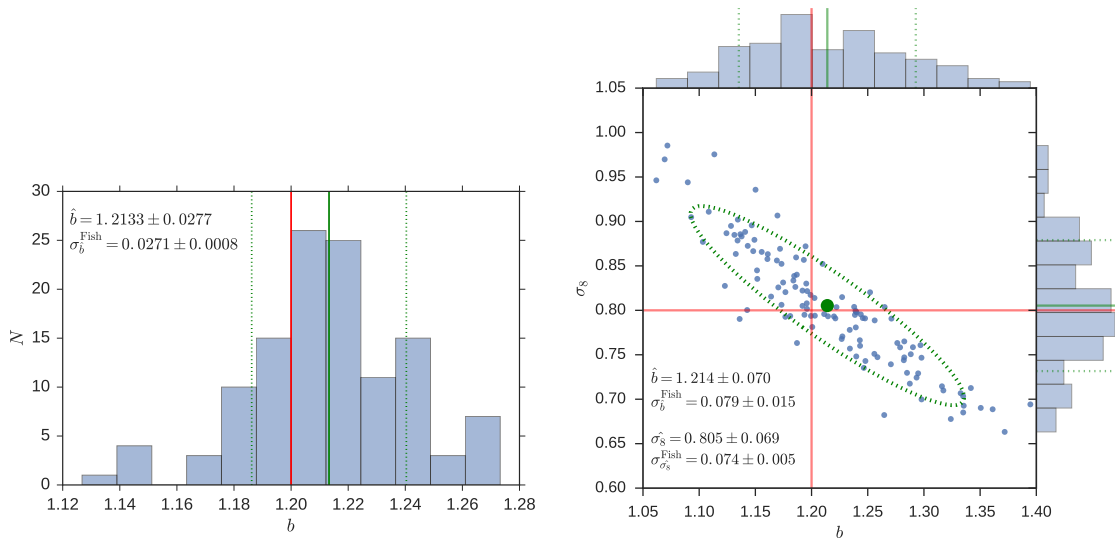


Figure 6. (Left) Distribution of the maximum-likelihood estimates of the bias, for the 120 realizations of the Las Damas mocks, for the case in which σ_8 is fixed. The vertical lines have the same meaning as in Figure 4. (Right) Distribution of the maximum-likelihood joint estimates of b and σ_8 , for these same mocks, for the case in which we fit for both parameters. The meaning of the different symbols and lines is the same as in Figure 5.

The recovered bias is compatible, within the errors, with the ‘true’ value. We note that we do not expect here a perfect agreement, as the input bias was fixed using a different statistic ($w_p(r_p)$) and range of scales.

The right panel of Figure 6 shows the 2D distribution of the estimates \hat{b} , $\hat{\sigma}_8$ when we also allow the power spectrum amplitude to vary. In this case, we obtain again results very similar to the ones obtained for the lognormal simulations. We obtain a relative error of the bias $\sigma_{\hat{b}}/\hat{b} = 5.8\%$, with the true dispersion being well recovered by the Fisher matrix estimate. We recover the amplitude of the power spectrum as $\hat{\sigma}_8 = 0.805 \pm 0.069$, in perfect agreement with the true value of $\sigma_8 = 0.8$. The Fisher matrix estimate of the uncertainty, $\sigma_{\sigma_8}^{\text{Fisher}} = 0.074 \pm 0.005$, slightly overestimates the error on $\hat{\sigma}_8$.

Overall, we obtain that the results for the Las Damas mocks are remarkably similar to those obtained for the case of the lognormal simulations and that the N-pdf method provides also in this case unbiased estimations of b and σ_8 . This is an indication that the basic assumptions of the method (lognormal distribution of the matter density field and linear biasing) are good enough approximations for our purposes in realistic distributions of galaxies, even if we now that they are not exact. In this way, we have validated the method, and we can confidently use it in real galaxy catalogues, as we do below.

4.2.1 Robustness with respect to the fiducial cosmological model

We also used the Las Damas mocks to assess how our results may depend on the assumed fiducial cosmology. We repeated the analysis for the 120 Las Damas mocks using three different cosmological models (in addition to the original one used above). We first tested the effect of changing the fiducial value of σ_8 alone. In this case, we kept all the rest of the cosmological parameters fixed to the true Las Damas cosmology, while changing the amplitude of the fiducial power spectrum. This results in a change of the covariance matrix \mathbf{C}_m used

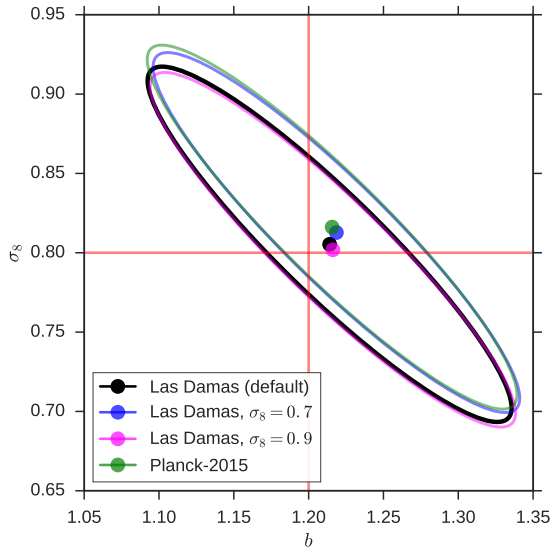


Figure 7. Average maximum-likelihood constraints on b , σ_8 , for the 120 Las Damas mock realisations, when assuming different fiducial cosmological models in the analysis. The black point and contour correspond to the true Las Damas cosmology and are the same as shown in the right panel of Figure 6. The blue and magenta colours correspond to the case in which we use the same Las Damas cosmology, except for the fiducial value of σ_8 . The green colour corresponds to the analysis performed assuming the *Planck-2015* cosmological parameters from [33].

in the analysis (see equation 2.15). We studied two cases, $\sigma_8^{\text{fid}} = 0.7, 0.9$, which encompass in excess the range of plausible values given our present knowledge [see, e.g., 33].

As a second test, we considered an overall change in all the cosmological parameters, and used the set of values compatible with the *Planck-2015* results that we use to analyse the real data. In addition to σ_8 , the main parameter potentially affecting our analysis is Ω_m , which changes from $\Omega_m = 0.25$ in the Las Damas cosmology to $\Omega_m = 0.308$ in the *Planck-2015* model. This change in parameters not only affects the covariance matrix \mathbf{C}_m used for the parameter estimation, but also the density field Δ_g itself (as we change the relation between redshifts and distances). For this test, therefore, we repeat the estimation of Δ_g with the new cosmology, following section 3.3.

We summarize our results (for the case in which we fit for both b and σ_8) in Figure 7 and Table 1. We see that, in all cases, the changes in the estimations of \hat{b} , $\hat{\sigma}_8$ are much smaller than the uncertainties. In the case of the galaxy bias, the maximum relative change with respect to the default analysis is 0.4%, while the relative error of the measurement is 5.8%. Regarding the recovered value of σ_8 , this relative change is 1.4%, compared to a relative error of 8.6%. The Fisher matrix estimation of the covariance matrix remains essentially unchanged for the different tested cosmologies. We can conclude, therefore, that our method is robust with respect to plausible changes in the fiducial cosmological model used in the analysis.

5 Results for SDSS data

We used the N-pdf method presented in section 2 to estimate the galaxy bias of the $M_r < -20$ sample and σ_8 using the galaxy density field Δ_g obtained from SDSS data as described

Fiducial cosmology	\hat{b}	$\sigma_{\hat{b}}^{\text{Fish}}$	$\hat{\sigma}_8$	$\sigma_{\hat{\sigma}_8}^{\text{Fish}}$
Las Damas	1.214 ± 0.070	0.079 ± 0.015	0.805 ± 0.069	0.074 ± 0.005
Las Damas, $\sigma_8 = 0.7$	1.219 ± 0.071	0.079 ± 0.015	0.813 ± 0.070	0.075 ± 0.005
Las Damas, $\sigma_8 = 0.9$	1.216 ± 0.071	0.079 ± 0.015	0.802 ± 0.069	0.074 ± 0.005
<i>Planck-2015</i>	1.216 ± 0.072	0.080 ± 0.016	0.816 ± 0.069	0.075 ± 0.005

Table 1. Results obtained for the maximum-likelihood estimates of the parameters (\hat{b} , $\hat{\sigma}_8$) and their Fisher-matrix uncertainties ($\sigma_{\hat{b}}$, $\sigma_{\hat{\sigma}_8}$), in the 120 Las Damas mocks, when using different fiducial cosmologies in the analysis, as explained in the text. In each case, we give the mean value and dispersion over the 120 realisations.

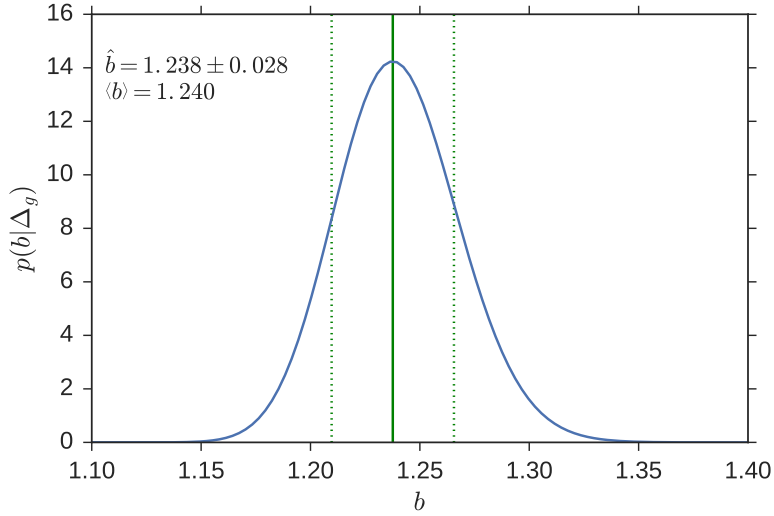


Figure 8. Posterior probability distribution of the bias parameter obtained by analysing the SDSS catalogue described in section 3.1, for the case in which σ_8 is fixed at its fiducial value, $\sigma_8^{\text{fid}} = 0.8149$. The solid vertical line marks the maximum-likelihood estimate \hat{b} , and the dashed lines correspond to the 1σ interval estimated from the Fisher matrix analysis.

in section 3.1. We first consider the case in which σ_8 is fixed at its fiducial value (here, $\sigma_8^{\text{fid}} = 0.8149$), and fit only for the galaxy bias. The posterior pdf of the bias in this case is shown in Figure 8, and the maximum-likelihood estimate obtained from the analysis is $\hat{b} = 1.238 \pm 0.028$. The mean bias is $\bar{b} = 1.240$.

This result can be compared to the bias estimated for the same SDSS sample by [11], using the projected correlation function $w_p(r_p)$. They obtained a value of $b = 1.20 \pm 0.01$ using HOD modelling, and $b = 1.17 \pm 0.07$ from the ratio of the galaxy and matter correlation functions in the range $r_p \in [4, 30] h^{-1} \text{ Mpc}$ (see their figure 7).⁶ There is a small discrepancy between these measurements and our results at only the $1 - 2\sigma$ level. This difference may just be due to the different methods used. As the range of scales used is also different (in our case, the scales probed are larger than the size of the cells, and therefore $\geq 30 h^{-1} \text{ Mpc}$), this

⁶These measurements correspond to $b = 1.18 \pm 0.01$ and $b = 1.15 \pm 0.07$, respectively, when we make the transformation from the fiducial value of σ_8 used in [11] to the one used here.

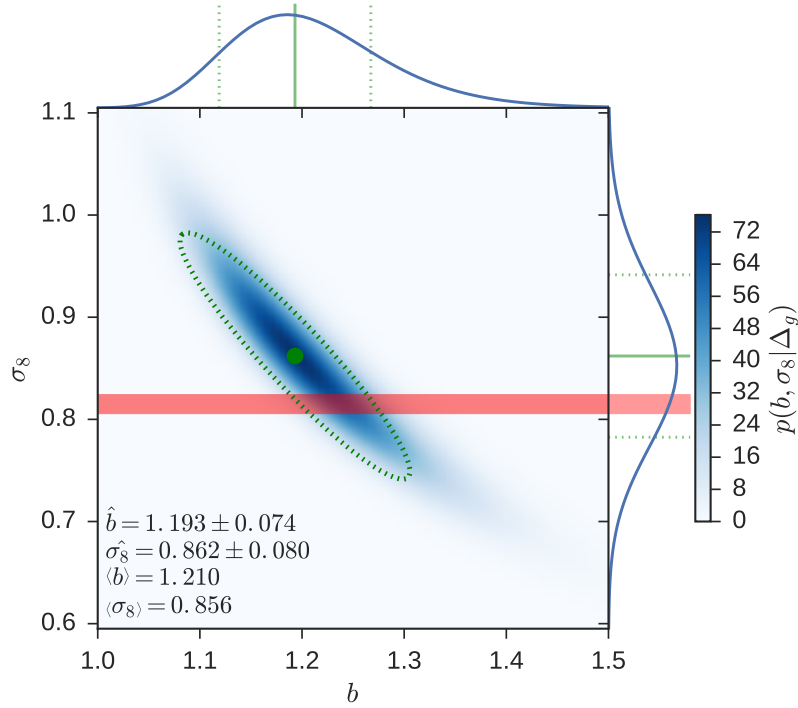


Figure 9. Joint posterior probability distribution of the two parameters b , σ_8 obtained by analysing the SDSS catalogue. The top and right sub-panels correspond to the marginalized probability distribution for each of the parameters separately. The green dot and dashed contour show the maximum-likelihood estimate of the parameters, and the 1σ confidence region obtained from the Fisher matrix analysis. The red horizontal band corresponds to the 1σ region from the measurement of σ_8 by *Planck-2015* [33]. We see that our constraints on σ_8 are fully compatible with the ones coming from CMB analysis.

could also be related to a scale dependent bias [59–62].

In Figure 9 we show the 2D joint posterior pdf for b and σ_8 for the case in which we fit for both parameters. The marginal posterior distributions are also shown at the top and right sides of the figure, respectively. The figure shows that we can indeed disentangle the constraints on the matter power spectrum from those on galaxy biasing. The corresponding maximum-likelihood estimates are $\hat{b} = 1.193 \pm 0.074$, $\hat{\sigma}_8 = 0.862 \pm 0.080$. From the Fisher matrix estimate of the covariance matrix, we derive the correlation coefficient between the parameters as $r = \frac{C_{12}}{\sigma_{\hat{b}}\sigma_{\hat{\sigma}_8}} = -0.937$

The bias estimate obtained from this analysis has a larger uncertainty than in the previous case (when σ_8 was fixed). However, it has the advantage of being an ‘absolute’ measurement, in the sense that it does not depend on choosing a particular value of σ_8 as is needed when using the usual 2-point clustering statistics.

From this analysis we also measure the amplitude of the matter power spectrum at the redshift of the survey ($z_{\text{med}} = 0.083$), which we express in terms of σ_8 . As shown in Figure 9, our measurement is in very good agreement with the value determined from *Planck-2015* data, $\sigma_8 = 0.8149 \pm 0.0093$ [33]. We measure σ_8 with a precision of 9%, which is far from the $\approx 1\%$ precision that can be achieved from CMB measurements. However, this measurement

Criterion	
AIC (H_0) – AIC (H_1)	12.6
BIC (H_0) – BIC (H_1)	8.22
GLRT : $\log\left(\frac{L_1}{L_0}\right)$ at $\nu = 1$	7.29

Table 2. Results of different model selection criteria (from top to bottom: *Akaike information criterion*, *Bayesian information criterion* and *generalized likelihood ratio test*) applied to the *null* hypothesis H_0 (bias is fixed at $b \equiv 1$, only σ_8 is allowed to vary), and the *alternative* hypothesis H_1 (both bias b and σ_8 are allowed to vary). The different criteria provide either ‘substantial’ or ‘strong’ evidence in favour of the biased model (H_1).

can be complementary as it is done using a different method at a very different redshift. It can be therefore used to test the consistency of the cosmological model, in a similar way as other low redshift estimates of σ_8 , e.g. via lensing [63, 64].

5.1 Model selection

We have shown that the N-pdf method breaks the degeneracy between the bias and the power spectrum amplitude using the shape of the distribution: it is lognormal for the matter density field, but differs from it (as described by equation 2.10) for the galaxy density field. We can assess how effective the method is to make this distinction using the model selection criteria described in section 2.3.

We compare two models. The *alternative* hypothesis H_1 is the model used elsewhere in the paper, in which both parameters (b , σ_8) are left free, and the *null* hypothesis H_0 is a model in which the value of galaxy bias is kept fixed at $b \equiv 1$, and σ_8 is the only free parameter. Hypothesis H_0 then corresponds to the case in which the N-pdf of the *galaxy* density field is lognormal (as that of matter), even if the clustering amplitude is allowed to change via σ_8 . We note that bias measurements relying on two-point statistics as the projected correlation function are unable to distinguish between these two models.

The results obtained, for the three criteria **AIC**, **BIC** and **GLRT** are presented in Table 2. The best-fit parameters obtained for hypothesis H_1 were presented in the previous section, in the case of H_0 we obtain $\hat{\sigma}_8 = 1.144 \pm 0.039$. As the **AIC** and **BIC** are approximations to the Bayes factors, we can use here the usual Jeffreys scale [65, 66] to assess the evidence of both models. According to that scale, the evidence against H_0 is ‘strong’ in the case of the **AIC**, and ‘substantial’ for the **BIC** (this difference comes from the fact that the **BIC** penalizes more heavily the addition of extra parameters). The **GLRT** also favours H_1 in a similar way. We can conclude from this test that the N-pdf of the galaxy density field does not follow a lognormal distribution, and it is better described by the biased model given by equation (2.10).

6 Conclusions and discussions

We have presented a full description of the N-probability density function of the galaxy number density fluctuations. The method follows the common assumption [e.g. 42, 43] that dark matter density fluctuations follow a local non-linear transformation of the initial energy density perturbations. The N-pdf of the galaxy number density fluctuations is given in terms

of the galaxy bias parameter and the cold dark matter correlations, parameterized, in our case, by its amplitude (σ_8).

The N-pdf provides us the most complete tool to perform statistical analyses, in particular parameter estimation and model selection. Regarding the former, optimal parameter estimation can be performed via the maximum-likelihood, since the N-pdf of the galaxy number density field, seen as a function of the bias and the σ_8 parameters, is nothing but the likelihood of the data (i.e., the galaxy number density realization) given these parameters. Even more, Bayesian inference can be also performed if any suitable information about the bias parameter is available in the form of a *prior*.

In relation to model selection, we have explored some well known criteria based on the likelihood (notice that, in the case of known priors, other approaches as Bayesian evidence, could be followed): the *Akaike information criterion*, the *Bayesian information criterion*, and the *generalized likelihood ratio test* (GLRT).

The methodology has been tested with SDSS-like simulations, both ideal log-normal realizations and mocks derived from the Las Damas project, showing, in both cases, that the maximum-likelihood estimates of the galaxy bias and the dark matter correlation amplitude are unbiased. We have applied our formalism to the 7th release of the SDSS main sample [50], for a volume-limited subset with magnitude $M_r < -20$. We obtain $\hat{b} = 1.193 \pm 0.074$ and $\hat{\sigma}_8 = 0.862 \pm 0.080$, for galaxy number density fluctuations in cells of the size of $30h^{-1}\text{Mpc}$. The \hat{b} and $\hat{\sigma}_8$ errors are obtained from the Fisher matrix. These are in good agreement with alternative estimates, as the mean bias and amplitude derived from the N-pdf.

The three model selection criteria mentioned above show that the *alternative* hypothesis (H_1 of a galaxy bias parameter b given by the maximum-likelihood estimator) is favoured with respect to a no-biasing scenario given by the *null* hypothesis H_0 of $b \equiv 1$.

Finally, we want to remark that our model assumes a constant bias over space, however the formalism can be generalized for a spatially varying bias. This is a more realistic situation, since it is well known that galaxy bias is scale-dependent and it evolves with redshift. This generalization is in progress, and will be addressed in a future paper.

Acknowledgements

We would like to thank an anonymous referee for his/her comments that have improved the quality and readability of this paper. We acknowledge partial financial support from the Spanish Ministry for Economy and Competitiveness and FEDER funds through grants AYA2010-22111-C03-02, AYA2012-39475-C02-01 and AYA2013-48623-C2-2, and Generalitat Valenciana project PrometeoII 2014/060. The authors acknowledge the computer resources, technical expertise and assistance provided by the Spanish Supercomputing Network (RES) node at Universidad de Cantabria. We thank the LasDamas collaboration for providing the mock catalogs that were used in this study.

Funding for the SDSS and SDSS-II has been provided by the Alfred P. Sloan Foundation, the Participating Institutions, the National Science Foundation, the U.S. Department of Energy, the National Aeronautics and Space Administration, the Japanese Monbukagakusho, the Max Planck Society, and the Higher Education Funding Council for England. The SDSS Web Site is <http://www.sdss.org/>.

The SDSS is managed by the Astrophysical Research Consortium for the Participating Institutions. The Participating Institutions are the American Museum of Natural History, Astrophysical Institute Potsdam, University of Basel, University of Cambridge, Case Western

Reserve University, University of Chicago, Drexel University, Fermilab, the Institute for Advanced Study, the Japan Participation Group, Johns Hopkins University, the Joint Institute for Nuclear Astrophysics, the Kavli Institute for Particle Astrophysics and Cosmology, the Korean Scientist Group, the Chinese Academy of Sciences (LAMOST), Los Alamos National Laboratory, the Max-Planck-Institute for Astronomy (MPIA), the Max-Planck-Institute for Astrophysics (MPA), New Mexico State University, Ohio State University, University of Pittsburgh, University of Portsmouth, Princeton University, the United States Naval Observatory, and the University of Washington.

References

- [1] D. G. York, J. Adelman, J. E. Anderson, Jr., S. F. Anderson, J. Annis, N. A. Bahcall, J. A. Bakken, R. Barkhouser, et al., *The Sloan Digital Sky Survey: Technical Summary*, *AJ* **120** (Sept., 2000) 1579–1587, [[astro-ph/0006396](#)].
- [2] M. Colless, G. Dalton, S. Maddox, W. Sutherland, P. Norberg, S. Cole, J. Bland-Hawthorn, T. Bridges, et al., *The 2dF Galaxy Redshift Survey: spectra and redshifts*, *Mon. Not. Roy. Astron. Soc.* **328** (Dec., 2001) 1039–1063, [[astro-ph/0106498](#)].
- [3] V. Springel, S. D. M. White, A. Jenkins, C. S. Frenk, N. Yoshida, L. Gao, J. Navarro, R. Thacker, et al., *Simulations of the formation, evolution and clustering of galaxies and quasars*, *Nature* **435** (June, 2005) 629–636, [[astro-ph/0504097](#)].
- [4] A. A. Klypin, S. Trujillo-Gomez, and J. Primack, *Dark Matter Halos in the Standard Cosmological Model: Results from the Bolshoi Simulation*, *Astrophys. J.* **740** (Oct., 2011) 102, [[arXiv:1002.3660](#)].
- [5] M. E. C. Swanson, M. Tegmark, M. Blanton, and I. Zehavi, *SDSS galaxy clustering: luminosity and colour dependence and stochasticity*, *Mon. Not. Roy. Astron. Soc.* **385** (Apr., 2008) 1635–1655, [[astro-ph/0702584](#)].
- [6] J. J. Condon, W. D. Cotton, E. W. Greisen, Q. F. Yin, R. A. Perley, G. B. Taylor, and J. J. Broderick, *The NRAO VLA Sky Survey*, *AJ* **115** (May, 1998) 1693–1716.
- [7] T. Jarrett, *Large Scale Structure in the Local Universe - The 2MASS Galaxy Catalog*, *PASA* **21** (2004) 396–403, [[astro-ph/0405069](#)].
- [8] B. Garilli, L. Guzzo, M. Scodeggio, M. Bolzonella, U. Abbas, C. Adami, S. Arnouts, J. Bel, et al., *The VIMOS Public Extragalactic Survey (VIPERS). First Data Release of 57 204 spectroscopic measurements*, *Astron. Astrophys.* **562** (Feb., 2014) A23, [[arXiv:1310.1008](#)].
- [9] S. P. Boughn and R. G. Crittenden, *Cross Correlation of the Cosmic Microwave Background with Radio Sources: Constraints on an Accelerating Universe*, *Physical Review Letters* **88** (Jan., 2002) 021302, [[astro-ph/0111281](#)].
- [10] C. L. Francis and J. A. Peacock, *Integrated Sachs-Wolfe measurements with photometric redshift surveys: 2MASS results and future prospects*, *Mon. Not. Roy. Astron. Soc.* **406** (July, 2010) 2–13, [[arXiv:0909.2494](#)].
- [11] I. Zehavi, Z. Zheng, D. H. Weinberg, M. R. Blanton, N. A. Bahcall, A. A. Berlind, J. Brinkmann, J. A. Frieman, et al., *Galaxy Clustering in the Completed SDSS Redshift Survey: The Dependence on Color and Luminosity*, *Astrophys. J.* **736** (July, 2011) 59–+, [[arXiv:1005.2413](#)].
- [12] C. Di Porto, E. Branchini, J. Bel, F. Marulli, M. Bolzonella, O. Cucciati, S. de la Torre, B. R. Granett, et al., *The VIMOS Public Extragalactic Redshift Survey (VIPERS). Measuring nonlinear galaxy bias at $z \sim 0.8$* , *ArXiv e-prints* (June, 2014) [[arXiv:1406.6692](#)].

- [13] J. N. Fry and E. Gaztanaga, *Biasing and hierarchical statistics in large-scale structure*, *Astrophys. J.* **413** (Aug., 1993) 447–452, [[astro-ph/9302009](#)].
- [14] E. Gaztanaga and J. A. Frieman, *Bias and high-order galaxy correlation functions in the APM galaxy survey*, *Astrophys. J. Let.* **437** (Dec., 1994) L13–L16, [[astro-ph/9407079](#)].
- [15] R. A. C. Croft, G. B. Dalton, and G. Efstathiou, *The APM cluster-galaxy cross-correlation function: constraints on Omega and galaxy bias*, *Mon. Not. Roy. Astron. Soc.* **305** (May, 1999) 547–562, [[astro-ph/9801254](#)].
- [16] Y. Sigad, E. Branchini, and A. Dekel, *Measuring the Nonlinear Biasing Function from a Galaxy Redshift Survey*, *Astrophys. J.* **540** (Sept., 2000) 62–73, [[astro-ph/0002170](#)].
- [17] C. Marinoni, O. Le Fèvre, B. Meneux, A. Iovino, A. Pollo, O. Ilbert, G. Zamorani, L. Guzzo, et al., *The VIMOS VLT Deep Survey. Evolution of the non-linear galaxy bias up to $z = 1.5$* , *Astron. Astrophys.* **442** (Nov., 2005) 801–825, [[astro-ph/0506561](#)].
- [18] K. Kovač, C. Porciani, S. J. Lilly, C. Marinoni, L. Guzzo, O. Cucciati, G. Zamorani, A. Iovino, et al., *The Nonlinear Biasing of the zCOSMOS Galaxies up to $z \sim 1$ from the 10k Sample*, *Astrophys. J.* **731** (Apr., 2011) 102, [[arXiv:0910.0004](#)].
- [19] P. Norberg, C. M. Baugh, E. Hawkins, S. Maddox, D. Madgwick, O. Lahav, S. Cole, C. S. Frenk, et al., *The 2dF Galaxy Redshift Survey: the dependence of galaxy clustering on luminosity and spectral type*, *Mon. Not. Roy. Astron. Soc.* **332** (June, 2002) 827–838, [[astro-ph/0112043](#)].
- [20] I. Zehavi, Z. Zheng, D. H. Weinberg, J. A. Frieman, A. A. Berlind, M. R. Blanton, R. Scoccimarro, R. K. Sheth, et al., *The Luminosity and Color Dependence of the Galaxy Correlation Function*, *Astrophys. J.* **630** (Sept., 2005) 1–27, [[astro-ph/0408569](#)].
- [21] P. Arnalte-Mur, V. J. Martínez, P. Norberg, A. Fernández-Soto, B. Ascaso, A. I. Merson, J. A. L. Aguerri, F. J. Castander, et al., *The ALHAMBRA survey: evolution of galaxy clustering since $z \sim 1$* , *Mon. Not. Roy. Astron. Soc.* **441** (June, 2014) 1783–1801, [[arXiv:1311.3280](#)].
- [22] H. Guo and Y. P. Jing, *Determine the Galaxy Bias Factors on Large Scales Using the Bispectrum Method*, *Astrophys. J.* **702** (Sept., 2009) 425–432, [[arXiv:0907.0282](#)].
- [23] J. E. Pollack, R. E. Smith, and C. Porciani, *A new method to measure galaxy bias*, *Mon. Not. Roy. Astron. Soc.* **440** (May, 2014) 555–576, [[arXiv:1309.0504](#)].
- [24] I. Szapudi, *Determining bias with cumulant correlators*, *Mon. Not. Roy. Astron. Soc.* **300** (Nov., 1998) L35–L38, [[astro-ph/9805090](#)].
- [25] L. Verde, A. F. Heavens, W. J. Percival, S. Matarrese, C. M. Baugh, J. Bland-Hawthorn, T. Bridges, R. Cannon, et al., *The 2dF Galaxy Redshift Survey: the bias of galaxies and the density of the Universe*, *Mon. Not. Roy. Astron. Soc.* **335** (Sept., 2002) 432–440, [[astro-ph/0112161](#)].
- [26] C. K. McBride, A. J. Connolly, J. P. Gardner, R. Scranton, R. Scoccimarro, A. A. Berlind, F. Marín, and D. P. Schneider, *Three-point Correlation Functions of SDSS Galaxies: Constraining Galaxy-mass Bias*, *Astrophys. J.* **739** (Oct., 2011) 85, [[arXiv:1012.3462](#)].
- [27] F.-S. Kitaura, J. Jasche, and R. B. Metcalf, *Recovering the non-linear density field from the galaxy distribution with a Poisson-lognormal filter*, *Mon. Not. Roy. Astron. Soc.* **403** (Apr., 2010) 589–604, [[arXiv:0911.1407](#)].
- [28] J. Jasche and F. S. Kitaura, *Fast Hamiltonian sampling for large-scale structure inference*, *Mon. Not. Roy. Astron. Soc.* **407** (Sept., 2010) 29–42, [[arXiv:0911.2496](#)].
- [29] J. Jasche and B. D. Wandelt, *Methods for Bayesian Power Spectrum Inference with Galaxy Surveys*, *Astrophys. J.* **779** (Dec., 2013) 15, [[arXiv:1306.1821](#)].

- [30] M. Ata, F.-S. Kitaura, and V. Müller, *Bayesian inference of cosmic density fields from non-linear, scale-dependent, and stochastic biased tracers*, *Mon. Not. Roy. Astron. Soc.* **446** (Feb., 2015) 4250–4259, [[arXiv:1408.2566](#)].
- [31] B. R. Granett, E. Branchini, L. Guzzo, U. Abbas, C. Adami, S. Arnouts, J. Bel, M. Bolzonella, et al., *The VIMOS Public Extragalactic Redshift Survey. Reconstruction of the redshift-space galaxy density field*, *Astron. Astrophys.* **583** (Nov., 2015) A61, [[arXiv:1505.06337](#)].
- [32] J. Jasche, F. Leclercq, and B. D. Wandelt, *Past and present cosmic structure in the SDSS DR7 main sample*, *JCAP* **1** (Jan., 2015) 36, [[arXiv:1409.6308](#)].
- [33] Planck Collaboration, P. A. R. Ade, N. Aghanim, M. Arnaud, M. Ashdown, J. Aumont, C. Baccigalupi, A. J. Banday, R. B. Barreiro, et al., *Planck 2015 results. XIII. Cosmological parameters*, *ArXiv e-prints* (Feb., 2015) [[arXiv:1502.01589](#)].
- [34] P. Vielva and J. L. Sanz, *Analysis of non-Gaussian cosmic microwave background maps based on the N -pdf. Application to Wilkinson Microwave Anisotropy Probe data*, *Mon. Not. Roy. Astron. Soc.* **397** (Aug., 2009) 837–848, [[arXiv:0812.1756](#)].
- [35] P. Vielva and J. L. Sanz, *Constraints on f_{NL} and g_{NL} from the analysis of the N -pdf of the CMB large-scale anisotropies*, *Mon. Not. Roy. Astron. Soc.* **404** (May, 2010) 895–907, [[arXiv:0910.3196](#)].
- [36] E. Komatsu and D. N. Spergel, *Acoustic signatures in the primary microwave background bispectrum*, *Phys. Rev. D* **63** (Mar., 2001) 063002, [[astro-ph/0005036](#)].
- [37] A. R. Liddle and D. H. Lyth, *Cosmological Inflation and Large-Scale Structure*. Cambridge University Press, Cambridge, UK, June, 2000.
- [38] W. C. Saslaw, *Thermodynamics and galaxy clustering - Relaxation of N -body experiments*, *Astrophys. J.* **297** (Oct., 1985) 49–60.
- [39] Y. Suto, M. Itoh, and S. Inagaki, *A gravitational thermodynamic approach to probe the primordial spectrum of cosmological density fluctuations*, *Astrophys. J.* **350** (Feb., 1990) 492–501.
- [40] O. Lahav, M. Itoh, S. Inagaki, and Y. Suto, *Non-Gaussian signatures from Gaussian initial fluctuations - Evolution of skewness and kurtosis from cosmological simulations in the highly nonlinear regime*, *Astrophys. J.* **402** (Jan., 1993) 387–397.
- [41] H. Ueda and J. Yokoyama, *Counts-in-cells analysis of the statistical distribution in an N -body simulated universe*, *Mon. Not. Roy. Astron. Soc.* **280** (June, 1996) 754–766, [[astro-ph/9501041](#)].
- [42] P. Coles and B. Jones, *A lognormal model for the cosmological mass distribution*, *Mon. Not. Roy. Astron. Soc.* **248** (Jan., 1991) 1–13.
- [43] I. Kayo, A. Taruya, and Y. Suto, *Probability Distribution Function of Cosmological Density Fluctuations from a Gaussian Initial Condition: Comparison of One-Point and Two-Point Lognormal Model Predictions with N -Body Simulations*, *Astrophys. J.* **561** (Nov., 2001) 22–34, [[astro-ph/0105218](#)].
- [44] A. Dekel and O. Lahav, *Stochastic Nonlinear Galaxy Biasing*, *Astrophys. J.* **520** (July, 1999) 24–34, [[astro-ph/9806193](#)].
- [45] M. Cacciato, O. Lahav, F. C. van den Bosch, H. Hoekstra, and A. Dekel, *On combining galaxy clustering and weak lensing to unveil galaxy biasing via the halo model*, *Mon. Not. Roy. Astron. Soc.* **426** (Oct., 2012) 566–587, [[arXiv:1203.2616](#)].
- [46] A. Lewis, A. Challinor, and A. Lasenby, *Efficient Computation of Cosmic Microwave Background Anisotropies in Closed Friedmann-Robertson-Walker Models*, *Astrophys. J.* **538** (Aug., 2000) 473–476, [[astro-ph/9911177](#)].

- [47] A. J. S. Hamilton, *Uncorrelated modes of the non-linear power spectrum*, *Mon. Not. Roy. Astron. Soc.* **312** (Feb., 2000) 257–284, [[astro-ph/9905191](#)].
- [48] H. Akaike, *Information theory and an extension of the maximum likelihood principle*, in *Proceeding of the Second International Symposium on Information Theory* (B. Petrov and F. Caski, eds.), (Budapest), pp. 267–281, Akademiai Kiado, 1973.
- [49] G. Schwarz, *Estimating the dimension of a model*, *The Annals of Statistics* **6** (03, 1978) 461–464.
- [50] K. N. Abazajian, J. K. Adelman-McCarthy, M. A. Agüeros, S. S. Allam, C. Allende Prieto, D. An, K. S. J. Anderson, S. F. Anderson, et al., *The Seventh Data Release of the Sloan Digital Sky Survey*, *ApJS* **182** (June, 2009) 543–558, [[arXiv:0812.0649](#)].
- [51] M. R. Blanton, D. J. Schlegel, M. A. Strauss, J. Brinkmann, D. Finkbeiner, M. Fukugita, J. E. Gunn, D. W. Hogg, et al., *New York University Value-Added Galaxy Catalog: A Galaxy Catalog Based on New Public Surveys*, *AJ* **129** (June, 2005) 2562–2578, [[astro-ph/0410166](#)].
- [52] A. J. S. Hamilton and M. Tegmark, *A scheme to deal accurately and efficiently with complex angular masks in galaxy surveys*, *Mon. Not. Roy. Astron. Soc.* **349** (Mar., 2004) 115–128, [[astro-ph/0306324](#)].
- [53] M. E. C. Swanson, M. Tegmark, A. J. S. Hamilton, and J. C. Hill, *Methods for rapidly processing angular masks of next-generation galaxy surveys*, *Mon. Not. Roy. Astron. Soc.* **387** (July, 2008) 1391–1402, [[arXiv:0711.4352](#)].
- [54] A. Labatie, J. Starck, M. Lachièze-Rey, and P. Arnalte-Mur, *Uncertainty in 2-point correlation function estimators and baryon acoustic oscillation detection in galaxy surveys*, *Statistical Methodology* **9** (Jan., 2012) 85–100, [[arXiv:1009.1232](#)].
- [55] M. Greiner and T. A. Enßlin, *Log-transforming the matter power spectrum*, *Astron. Astrophys.* **574** (Feb., 2015) A86, [[arXiv:1312.1354](#)].
- [56] V. J. Martínez and E. Saar, *Statistics of the Galaxy Distribution*. Chapman & Hall/CRC, Boca Raton, 2002.
- [57] C. McBride, A. Berlind, R. Scoccimarro, R. Wechsler, M. Busha, J. Gardner, and F. van den Bosch, *LasDamas Mock Galaxy Catalogs for SDSS*, in *American Astronomical Society Meeting Abstracts #213*, vol. 41 of *Bulletin of the American Astronomical Society*, p. 253, Jan., 2009.
- [58] E. A. Kazin, M. R. Blanton, R. Scoccimarro, C. K. McBride, A. A. Berlind, N. A. Bahcall, J. Brinkmann, P. Czarapata, et al., *The Baryonic Acoustic Feature and Large-Scale Clustering in the Sloan Digital Sky Survey Luminous Red Galaxy Sample*, *Astrophys. J.* **710** (Feb., 2010) 1444–1461, [[arXiv:0908.2598](#)].
- [59] L.-Z. Fang, Z.-G. Deng, and X.-Y. Xia, *Detecting Scale-Dependence of Bias from APM-BGC Galaxies*, *Astrophys. J.* **506** (Oct., 1998) 53–63, [[astro-ph/9805238](#)].
- [60] M. Blanton, R. Cen, J. P. Ostriker, and M. A. Strauss, *The Physical Origin of Scale-dependent Bias in Cosmological Simulations*, *Astrophys. J.* **522** (Sept., 1999) 590–603, [[astro-ph/9807029](#)].
- [61] P. Coles and P. Erdogdu, *Scale dependent galaxy bias*, *JCAP* **10** (Oct., 2007) 7, [[arXiv:0706.0412](#)].
- [62] V. Desjacques and R. K. Sheth, *Redshift space correlations and scale-dependent stochastic biasing of density peaks*, *Phys. Rev. D* **81** (Jan., 2010) 023526, [[arXiv:0909.4544](#)].
- [63] H. Hoekstra, H. K. C. Yee, and M. D. Gladders, *Constraints on Ω_m and σ_8 from Weak Lensing in Red-Sequence Cluster Survey Fields*, *Astrophys. J.* **577** (Oct., 2002) 595–603, [[astro-ph/0204295](#)].

- [64] M. J. Jee, J. A. Tyson, M. D. Schneider, D. Wittman, S. Schmidt, and S. Hilbert, *Cosmic Shear Results from the Deep Lens Survey. I. Joint Constraints on Ω_M and σ_8 with a Two-dimensional Analysis*, *Astrophys. J.* **765** (Mar., 2013) 74, [[arXiv:1210.2732](#)].
- [65] H. Jeffreys, *Theory of Probability*. Oxford University Press, Oxford, UK, 1961.
- [66] R. E. Kass and A. E. Raftery, *Bayes factors*, *Journal of the American Statistical Association* **90** (1995), no. 430 773–795.